Catalytic combustion of methane over barium hexaferrites

A. Favre [a], N. Guilhaume [a,*], J.-M.M. Millet [b] and M. Primet [a]

[a] *Laboratoire d'Application de la Chimie à l'Environnement, UMR CNRS 5634, Université Claude Bernard Lyon I, Bât. 303, 43 Boulevard du 11 Novembre 1918, F-69622 Villeurbanne Cedex, France*
E-mail: guilhau@cpmol.univ-lyon1.fr
[b] *Institut de Recherches sur la Catalyse, 2 Avenue Albert Einstein, F-69626 Villeurbanne Cedex, France*

Received 22 July 1997; accepted 17 October 1997

Barium hexaferrite $BaFe_{12}O_{19}$ and iridium-containing barium hexaferrites have been prepared by the citrates gel method. Their catalytic activity in methane combustion has been evaluated. $BaFe_{12}O_{19}$ is an efficient catalyst for this reaction, and the introduction of iridium in the hexaferrite structure does not improve this activity. Mössbauer spectroscopy suggests that a part of the iridium ions are incorporated in the hexaferrite structure, however in crystallographic sites where they cannot interact with the gas phase. Infrared study of CO adsorption reveals the presence of two types of iridium particles in the surface: small Ir particles, in strong interaction with the hexaferrite structure, and some larger Ir particles which were not incorporated into the lattice.

Keywords: catalytic combustion, methane combustion, barium hexaferrite, iridium substitution, Mössbauer spectroscopy

1. Introduction

The catalytic combustion of methane, the major component of natural gas, has received considerable attention in the past years, because it allows the production of energy without nitrogen oxides formation. Noble metal-based catalysts, in particular Pt, Pd and Ir, are the most active for the oxidation of saturated hydrocarbons. Transition metal oxides, and among them copper and manganese oxides, also show good activity, although at higher temperatures [1]. In view of high temperatures applications like gas turbines, the resistance to sintering (leading to growth of particles, lowering of surface areas and eventually reaction between the active phase and the support) is a crucial problem for both types of catalysts.

An interesting approach to this problem has been developed by Arai and co-workers: they introduced catalytically active transition metal cations (Cr, Mn, Fe, Ni) [2] in the lattice of barium hexaaluminate, which shows exceptional resistance to sintering at high temperatures. This allows the stabilisation of the active phase by incorporation into the lattice of a high-temperature resistant matrix.

By analogy with barium hexaaluminates, we investigated the catalytic properties of barium hexaferrite $BaFe_{12}O_{19}$, in the combustion of methane. Iron oxide Fe_2O_3, and the perovskite $LaFeO_3$, are known as active catalysts, although not the most ones, for methane total oxidation [3,4]. Very recently, the activity of iron-substituted barium hexaferrites $BaFe_xAl_{(12-x)}O_{19}$ and of $BaFe_{12}O_{19}$ have been reported, and their thermal stability evaluated [5]. We chose to substitute a small part of iridium for iron in the hexaferrite structure, since iridium is one of the most active metals for methane combustion, but the high volatility of its oxides prevents its use in this high-temperature reaction. Incorporation of iridium in an oxide lattice can be expected to improve the activity for hydrocarbons combustion, and to stabilise the iridium against volatilisation.

2. Experimental

The catalysts were prepared by the citrate-gel method: the required amounts of barium acetate and iron nitrate were dissolved in water. In the case of the Ir-containing catalysts, an acetone solution of iridium acetylacetonate was added to this aqueous solution. The metal cations were complexed by citric acid (two moles/positive charge), and the pH was adjusted to 6 by addition of ammonia. The solution was slowly evaporated by heating until a viscous gel was formed. Three samples were prepared, one free of iridium $BaFe_{12}O_{19}$ (sample A), and two solids in which 1 and 5 wt% Ir were introduced in substitution of iron. The amounts of iridium correspond to the theoretical formulas $BaFe_{11.942}Ir_{0.058}O_{19}$ (sample B) and $BaFe_{11.70}Ir_{0.30}O_{19}$ (sample C) respectively.

The gels were first calcined at 450°C in a muffle furnace (heating rate 2°C/min) for 2 h, in order to decompose the metal salts and the organic gel. The resulting solid was crushed and calcined again at 900°C in a quartz cell under flowing air, for 3 h (heating rate 2°C/min).

Specific surface areas were measured by nitrogen adsorption on samples previously desorbed at 300°C under vacuum (5×10^{-5} Torr).

Powder X-ray diffraction patterns were recorded with a D 500 Siemens diffractometer using monochromatised Cu Kα radiation. The patterns were recorded from 3° to

* To whom correspondence should be addressed.

70° 2θ with a scan rate of 1.2° min^{-1}, and were compared with the ICDD reference data file for phase identification.

Transmission electron microscopy, coupled with EDX analysis, was performed with a Jeol 2010 electron microscope operating at 200 eV.

The Mössbauer spectra were recorded at room temperature, using a 2 GBq $^{57}Co/Rh$ source and a conventional constant acceleration spectrometer, operated in triangular mode. The samples were diluted in Al_2O_3 in order to avoid a too high Mössbauer absorption, and pressed into pellets. The isomer shifts (δ) were given with respect to α-Fe and were calculated, as the quadrupole splittings (Δ) and the line width (W), with a precision of about 0.02 mm s^{-1}. The accuracy for hyperfine fields (H) determinations was 5 kOe.

Infrared study of CO adsorption was performed with a Nicolet Magna 550 FTIR spectrometer. The samples (40–50 mg) were pressed into thin disks and introduced into a cell allowing in situ treatments at various temperatures. Each spectrum corresponds to the accumulation of 100 scans. The spectral range observed is 4000–400 cm^{-1}, with a resolution of 4 cm^{-1}. In the spectra presented the gas phase was always evacuated.

The catalytic activity was measured in isothermal conditions, in the temperature range 350–800°C. The conditions of the tests have been described in detail previously [6]. The reactant gas mix consisted of 1 vol% CH_4, 4 vol% O_2 and N_2 as balance, with a total flow rate of 6.4 $\ell\,h^{-1}$. The catalysts were loaded in a quartz reactor and pre-treated under oxygen at 400°C for 1 h. The temperature was cooled down to 350°C, and the reactant gases were admitted into the reactor. The amount of catalyst used was 0.50 g, corresponding to a space velocity around 5000 h^{-1} for the three solids.

3. Results

3.1. Preparation and physico-chemical characterisations

The diffraction pattern of the most Ir-loaded catalyst $BaFe_{11.70}Ir_{0.30}O_{19}$ (C) is shown in figure 1. The three catalysts, after calcination at 900°C, present similar patterns corresponding to the reference phase $BaFe_{12}O_{19}$ (ICDD 39-1433). No other phase was detected, while after calcination at 700°C the solids were still polyphasic and contained Fe_2O_3.

In the case of the two iridium-containing samples (B and C), no displacement of the diffraction lines due to Ir incorporation can be noticed. Cell parameters calculated from powder diffraction patterns (table 1) do not differ much from those given in the ICDD reference data file for the $BaFe_{12}O_{19}$ phase. However, this is not surprising since the effective ionic radii of Fe^{3+} and Ir^{4+} are very similar, 0.645 and 0.625 Å respectively [7], and the amounts of iridium introduced (1 and 5 wt%) correspond to low Ir/Fe atomic ratios. It must be noticed that, although the oxidation state of iridium in the $Ir(acac)_3$ precursor was Ir^{3+}, it is expected to be found as Ir^{4+} when incorporated in the $BaFe_{12}O_{19}$ phase, because Ir^{4+} is the most stable oxidation state of iridium in an oxide lattice [8].

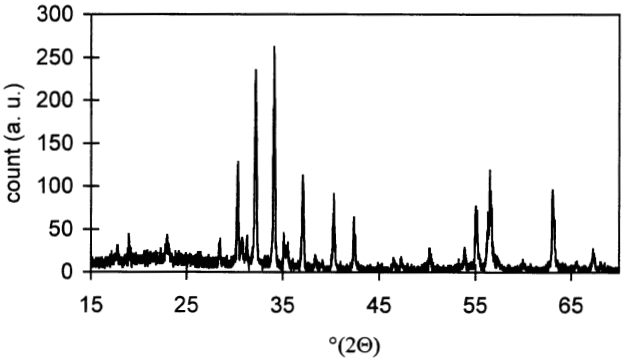

Figure 1. X-ray diffraction pattern of sample C.

The chemical analyses gave satisfactory results for barium and iron; however, the iridium content analysed was about ten times lower than expected, which suggests that a partial loss of iridium oxide may have occurred upon calcination at 900°C.

TEM examination of the most Ir-loaded catalyst C (5 wt% Ir in theory) reveals well crystallised particles of uniform size and shape. EDX analysis confirms the presence of iridium uniformly distributed in all analysed particles, however in a smaller amount than expected (0.5–1 wt%). A partial loss of Ir upon calcination at 900°C thus cannot be excluded.

The specific surface areas of the three catalysts (table 1) are close, around 10 $m^2\,g^{-1}$, after calcination at 900°C.

3.2. Catalytic activity in methane combustion

The conversions of methane in isothermal conditions, in the temperature domain 350–800°C, are reported in figure 2. The first point worth noticing is the high activity of the three samples, the conversion starting at 350°C, and being total at 700°C. The only product detected is

Table 1
Specific surface areas and unit cell parameters of the $BaFe_{12}O_{19}$ (A), $BaFe_{11.942}Ir_{0.058}O_{19}$ (B) and $BaFe_{11.70}Ir_{0.30}O_{19}$ (C) catalysts, after calcination at 900°C

Catalyst	Surface area ($m^2\,g^{-1}$)	Unit cell parameters (Å)	
		a	c
A	9.1	5.889(3)	23.21(1)
B	11	5.887(3)	23.19(1)
C	11	5.890(2)	23.22(1)
$BaFe_{12}O_{19}$ (ICDD 39-1433)	–	5.8945(5)	23.215(3)

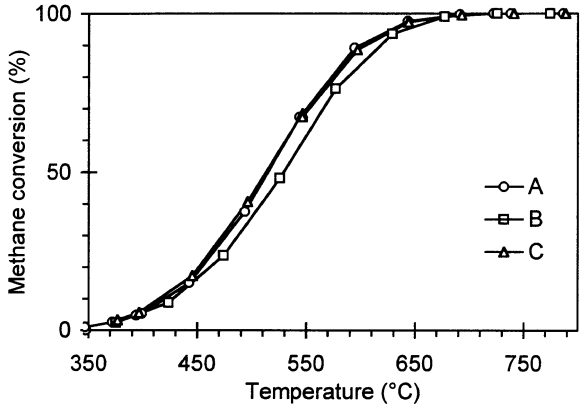

Figure 2. Methane conversion versus temperature, for the three catalysts A, B and C. Feed: 1 vol% CH_4, 4 vol% O_2, balance N_2; SV: 5000 h^{-1}.

carbon dioxide in the whole temperature range. It appears that the three catalysts behave similarly, and that the introduction of iridium has no influence on the activity. The apparent activation energy is slightly lower in the case of catalyst C (94 kJ mol^{-1}, to compare with 98 kJ mol^{-1} for catalysts A and B); however, this difference cannot be considered as really significant. Activity expressed as μmole methane transformed per minute and per gram catalyst (table 2) in the low conversions domain (< 20%) confirms this observation: the unsubstituted ferrite $BaFe_{12}O_{19}$ has the same activity as the solid containing theoretically 5 wt% Ir. EDX analysis showed that the most Ir-loaded catalyst C contained iridium, however in smaller amounts than expected. As iridium oxides are volatile, the question that raised was whether the Ir- substituted catalysts B and C contained iridium in surface, which could have been lost upon calcination, and, if present, why it has no influence on the activity of the hexaferrite.

3.3. Localisation of iridium in the hexaferrite structure

3.3.1. Mössbauer spectroscopy

The ^{57}Fe Mössbauer absorption spectrum of the barium hexaferrite has been fully interpreted [9,10]. It has been fitted at room temperature to four sextets corresponding to the five crystallographic sites, listed in table 3 (from ref. [11]), of the structure. The $4f_{IV}$ and 2a sites, presenting approximately the same magnetic hyperfine field at room temperature, could not be fitted

Table 2
Activity at 400 and 450°C, expressed as μmoles CH_4 transformed per minute and per gram catalyst (μmol-CH_4 min^{-1} g^{-1})

Catalyst	Activity at 400°C	Activity at 450°C
A	4.5	15.4
B	4.1	13.5
C	5.3	17.0

Table 3
Coordination of iron and number of Fe^{3+} cations in the five iron sublattices of the $BaFe_{12}O_{19}$ structure (from ref. [11])

Site	Coordination	Number of ions	Block [a]
12k	octahedral	6	R/S
$4f_1$	tetrahedral	2	S
$4f_2$	octahedral	2	R
2a	octahedral	1	S
2b	fivefold	1	R

[a] R = hexagonal block, S = spinel block.

with two distinct sextets. The relative intensities of the observed sextets (table 4) were in good agreement with the relative abundance of the sites.

The spectra of the Ir-doped compounds did not present important changes. The spectra could always be fitted to the same four sextets. No Fe^{2+} were detected, the charge balance corresponding to the substitution of Fe^{3+} by Ir^{4+} should thus be achieved by an electron delocalization. Only the spectrum of the most Ir-loaded catalyst C is presented in figure 3, as the three samples A, B and C have identical spectra, with only a slight difference in the relative intensities of the sextets (table 4). Figure 4, from the data of table 4, shows clearly the decrease of the relative intensity of the $(2a + 4f_1)$ sextet when the amount of iridium introduced increases, suggesting that the iridium is located in these positions in replacement of iron. Since the coordination in the $4f_1$ position is tetrahedral, which is not favoured in the case of Ir^{4+} (d^5), we suppose that the iridium ions are preferentially located in the octahedral 2a positions. The preferential substitution of the 2a sites in barium hexaferrites has been early reported when the substituent was, as Ir^{4+}, a smaller and more electropositive cation like Al^{3+} [12,13]. These sites, as well as the $4f_1$ sites, are located in the middle of the spinel block [11], surrounded by iron ions in a compact packing, which means that most of the iridium introduced in the structure is not accessible to the gas phase. This can be a reason for the lack of influence of the iridium doping on the catalytic activity in methane oxidation.

It can be noticed that when iridium was substituted for iron in barium hexaferrites for applications as materials for magnetic devices, the substitution was coupled with that of a bivalent cation, Co^{2+} or Zn^{2+} [14]. Refinements of the structures showed that the Co^{2+} and

Table 4
Relative intensities (%) of the four Mössbauer sextets corresponding to the different crystallographic sites of the hexaferrite structure, for samples A, B and C

Site	A	B	C
$4f_2$	19.3	21	21
$2a + 4f_1$	29.6	28	22
12k	47	48	52
2b	4.1	4	4

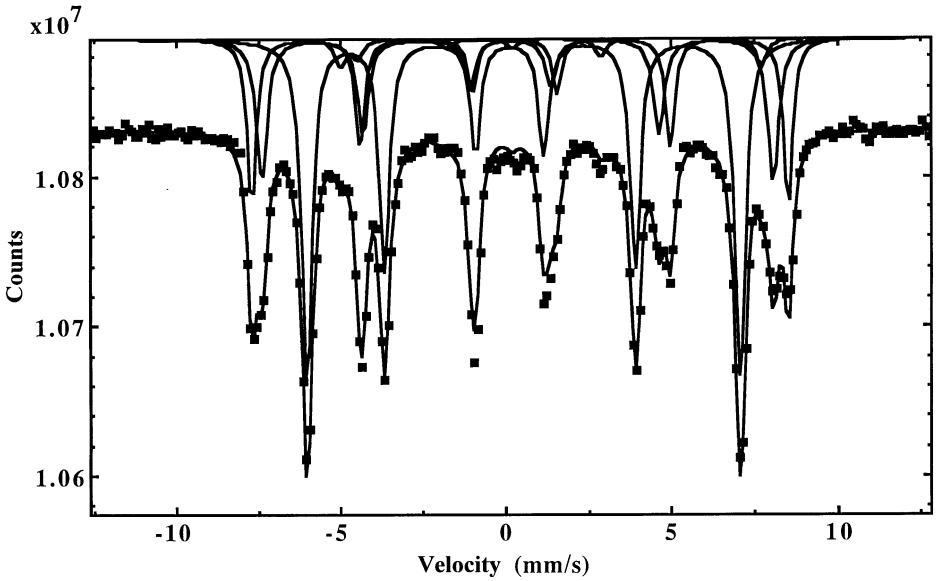

Figure 3. ^{57}Fe-Mössbauer spectrum of the $BaFe_{11.70}Ir_{0.30}O_{19}$ catalyst (C) at room temperature. (■) Experimental spectrum; full lines: four sextets fitting the experimental spectrum.

Zn^{2+} cations occupy preferentially the $4f_1$ (T_d) and 2b (O_h) sites of the spinel block, and in this case the iridium becomes preferentially distributed in the 12k and $4f_2$ positions, which should be more interesting for catalytic activity because they belong to the limit of the R/S and R blocks respectively. This opens the possibility of controlling the position of the active ion by the appropriate choice of the substituents in the structure.

3.3.2. Infrared study of CO adsorption

No adsorption was observed on sample A containing no iridium. According to the literature, CO adsorption on Fe^{3+} is weak, reversible, and observed only at low temperature (77 K): it appears as a strong band at 2165.5 cm^{-1} [15], this frequency higher than gaseous CO (2143 cm^{-1}) revealing a simple σ-dative bond.

The infrared spectrum of CO adsorbed at ambient temperature on catalyst C is depicted in figure 5 (on sample B, the same bands are observed, but they are weaker). These bands correspond thus to the adsorption of CO on iridium, and as expected they are stronger in the case of the most Ir-loaded solid $BaFe_{11.70}Ir_{0.30}O_{19}$. Two intense bands can be noticed at 2012 cm^{-1} (with a shoulder at 2045 cm^{-1}) and 1798 cm^{-1}.

Several authors have studied the adsorption of CO on metallic iridium particles deposited on either alumina or silica [16–18]: they agree on the fact that it leads to νCO bands in the following frequency domains: (i) 2060–2080 cm^{-1} (CO adsorbed on large iridium particles, in which the Ir atoms accessible to the gas phase have no interaction with the support); (ii) 2010–2030 cm^{-1} (CO adsorbed on isolated, small Ir clusters, in strong interaction with the support), and (iii) 1850 cm^{-1} (CO bridging two Ir atoms, this band is not always observed).

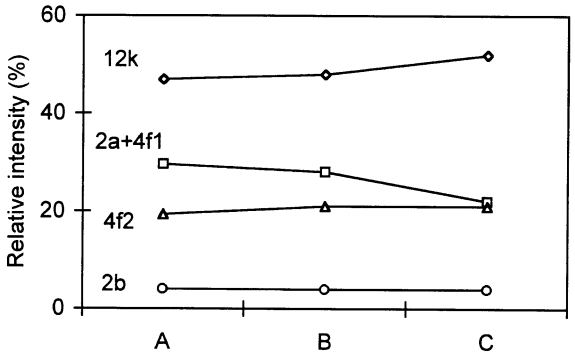

Figure 4. Relative intensities of the four Mössbauer sextets for samples A, B and C.

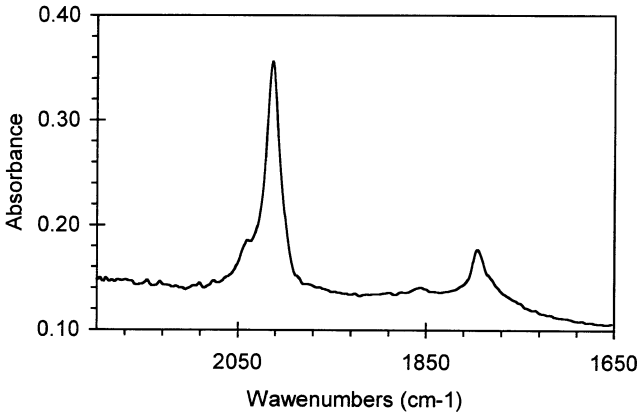

Figure 5. IR spectrum of CO irreversibly adsorbed at room temperature on sample C, previously desorbed at 400°C.

The three bands that we observe in the same frequency domains can be attributed to two types of iridium particles: the intense band at 2012 cm^{-1} should correspond to CO adsorbed on small iridium particles, in strong interaction with the hexaferrite structure. It should be the only band observed if iridium was totally dispersed in the oxide. However, the presence of the 2045 and the 1798 cm^{-1} (bridging CO) bands suggest the presence of larger iridium particles: they indicate that a fraction of the iridium is not incorporated in the ferrite, which is not homogeneously dispersed in the structure.

The bands observed correspond in all cases to CO adsorbed on iridium in a *reduced* state, while the catalysts are supposed to contain iridium cations Ir^{4+}. This reduction of surface iridium ions can occur under vacuum at 400°C, or by reaction with CO leading to the formation of CO_2 and reduced metal.

This study of CO adsorption confirms the presence of iridium at the surface of samples B and C, in a larger amount in the case of C. However, it cannot be quantified. It should be remembered that the preparation method involves that only a small part of the iridium introduced is present at the surface of the samples, the main part being distributed in the whole catalyst mass. Iridium is not homogeneously incorporated in the hexaferrite lattice: large iridium particles are formed in addition to the expected Ir sites incorporated in the oxide lattice. This is probably another reason for the non-influence of iridium on the activity of the substituted catalysts in comparison to $BaFe_{12}O_{19}$.

4. Conclusion

Barium hexaferrite $BaFe_{12}O_{19}$ is an efficient catalyst for methane combustion. We tried to introduce iridium ions in this mixed-oxide structure, in order to improve the low temperature performances of the solids, and to stabilise iridium against volatilisation.

The partial substitution of iridium for iron does not improve the activity of the catalysts in this reaction. This is explained in view of surface and bulk physico-chemical characterisations of the solids:

– A partial loss of iridium upon calcination of the samples at 900°C is probable, as chemical and EDX analysis detect smaller iridium amounts than expected from the synthesis.

– Mössbauer spectroscopy showed that the iridium ions incorporated in the hexaferrite structure are probably located in the 2a sites, inside the spinel blocks, and thus not easily accessible to the gas phase.

– Infrared study of adsorbed CO reveals that some surface iridium is accessible for CO chemisorption, but it is not homogeneously distributed in the hexaferrite structure: in addition to the expected isolated iridium sites, some larger, sintered, iridium particles are present, which are not incorporated in the oxide lattice.

The substitution of iridium for iron appeared to be very limited. This may be due to the fact that the charge of Ir^{4+} in the lattice could not be balanced by Fe^{2+} cations, but only by electron delocalization, which should remain limited in the hexaferrite structure.

References

[1] R. Prasad, L.A. Kennedy and E. Ruckenstein, Catal. Rev. Sci. Eng. 26 (1984) 1.
[2] M. Machida, K. Eguchi and H. Arai, J. Catal. 120 (1989) 377.
[3] J.G. McCarty and H. Wise, Catal. Today 8 (1990) 231.
[4] T. Seiyama, Catal. Rev. Sci. Eng. 34 (1992) 281.
[5] G. Groppi, C. Cristiani and P. Forzatti, J. Catal. 168 (1997) 95.
[6] N. Guilhaume and M. Primet, J. Chem. Soc. Faraday Trans. 90 (1994) 1541.
[7] R.D. Shannon, Acta Cryst. A 32 (1976) 751.
[8] D.-Y. Jung, G. Demazeau, J. Etourneau and M.A. Subramanian, Mater. Res. Bull. 30 (1995) 113.
[9] J.S. Van Wieringen and J.G. Rensen, Z. Anorg. Phys. 21 (1966) 69.
[10] A.H. Morrish, X.Z. Zhou, Z. Yang and H.X. Zeng, Hyperfine Interactions 90 (1994) 365.
[11] G. Albanese, J. Phys. 38 (C1) (1977) 85.
[12] G. Albanese, G.Asti and P. Batti, Nuovo Cimento 58B (1968) 480.
[13] E.F. Beraut, A. Deschamps, R. Pauthenet and S. Pickart, J. Phys. Radium 20 (1959) 404.
[14] H. Vincent, E. Brando and B. Sugg, J. Solid State Chem. 120 (1995) 17.
[15] A. Zecchina, D. Scarano and A. Reller, J. Chem. Soc. Faraday Trans. I 84 (1988) 2327.
[16] R.F. Howe, J. Catal. 50 (1977) 196.
[17] F. Solymosi and J. Rasko, J. Catal. 62 (1980) 253.
[18] F.J.C.M. Toolenaar, G.J. van der Poort, F. Stoop and V. Ponec, J. Chim. Phys. 78 (1981) 927.